

The Copycat Perceptron: Smashing Barriers Through Collective Learning

Giovanni Catania,¹ Aurélien Decelle,^{1,2} and Beatriz Seoane²

¹*Departamento de Física Teórica, Universidad Complutense de Madrid, 28040 Madrid, Spain*

²*Université Paris-Saclay, CNRS, INRIA Tau team, LISN, 91190 Gif-sur-Yvette, France.*

We characterize the equilibrium properties of a model of y coupled binary perceptrons in the teacher-student scenario, subject to a suitable learning rule, with an explicit ferromagnetic coupling proportional to the Hamming distance between the students' weights. In contrast to recent works, we analyze a more general setting in which a thermal noise is present that affects the generalization performance of each student. Specifically, in the presence of a nonzero temperature, which assigns nonzero probability to configurations that misclassify samples with respect to the teacher's prescription, we find that the coupling of replicas leads to a shift of the phase diagram to smaller values of α : This suggests that the free energy landscape gets smoother around the solution with good generalization (i.e., the teacher) at a fixed fraction of reviewed examples, which allows local update algorithms such as Simulated Annealing to reach the solution before the dynamics gets frozen. Finally, from a learning perspective, these results suggest that more students (in this case, with the same amount of data) are able to learn the same rule when coupled together with a smaller amount of data.

I. INTRODUCTION

Statistical mechanics offers a valuable approach to understanding learning problems. It accomplishes this by characterizing the neural network's phase diagram based on global parameters such as the number of data points or the inherent noise of the gradient descent dynamics [1, 2]. This method has demonstrated a deep understanding of the conditions necessary for the learning algorithm to perform better and achieve effective generalization solutions, and also identify when a good performance is simply impossible. A remarkable illustration of the power of this strategy lies in the characterization of the solution space as a function of the proportion of clauses for the K-SAT [3], a paradigmatic combinatorial optimization problem, or in the so-called colouring problems [4, 5].

At zero temperature, the task of accurately classifying a labeled data set with random labels can be formulated as a constraint satisfaction problem (CSP). Examples range from perceptrons [6, 7], or more complex architectures such as the Committee Machine [8, 9], Support Vector Machines [10], multilayered perceptrons for binary [11] or multiclass supervised tasks [12], or even other continuous optimization problems in condensed matter, such as the jamming transition [13]. In practice, this means that finding "good" solutions among the multitude of possibilities with poor generalization should be an enormous challenge. Contrary to this intuition, perceptrons and deep neural networks show exceptional performance on classification tasks. This evidence highlights that standard training algorithms do not exhaustively explore the entire space of quasi-optimal solutions of the CSP, but do something more efficient.

In recent years, researchers have introduced a theoretical framework based on the concept of *local entropy* to gain better insight into the success of training algorithms and to effectively find solutions that exhibit good generalization. This concept, along with the coupled-replicas strategy, has been thoroughly investigated in sev-

eral studies [14–17]. In addition, a recent work [18] has provided convincing evidence that coupling replicas can help in identifying favorable local minima and avoiding entrapment in glassy states, as illustrated in the graph coloring problem.

In this study, we focus on the paradigmatic example of the binary perceptron model in the so-called *teacher-student scenario*: a "student" perceptron tries to learn the rule to correctly classify the examples provided (and previously classified) by the teacher. In contrast to the storage problem, where one is interested in characterizing the typical solutions' volume and its geometric organization (e.g., whether it is connected or disconnected), possibly leading to a SAT /UNSAT transition at a critical value of load α , in the teacher student scenario α plays a role similar to a signal-to-noise ratio, since there is always at least one solution (i.e., the teacher's), therefore defining a "planted" problem [19]. In contrast to perceptrons with continuous variables, where generalization performance gradually improves as the amount of data increases in a continuous fashion, the binary perceptron exhibits a more intriguing behavior. In the thermodynamic limit, it undergoes a first-order phase transition that leads to a sudden drop in the generalization error towards zero as the number of training examples increases.

The binary perceptron problem has been the subject of investigation for decades, with researchers mainly using techniques from statistical physics, in particular spin-glass theory. Early research focused on determining its storage capacity [6, 20, 21]. Other previous works also tried to understand the properties of its generalization error in the teacher-student scenario [22–24]. Several learning rules were explored as part of these studies. More recently, a large deviation approach has been used to characterize the properties of the solution space near the critical point. This approach uses the aforementioned local entropy formalism [15, 17, 25] and has shown promising results.

The local entropy formalism is closely related to the

Franz-Parisi potential in glassy physics [26, 27]. This potential serves as a valuable tool for analyzing the probability of finding alternative solutions in the vicinity of a given reference configuration [28, 29], thus allowing the structure of the solution space to be studied. The construction of the Franz-Parisi potential involves an extended ensemble of two or more replicas of the same model, all coupled together via a field γ , with the goal of favoring configurations where the replicas are similar. In our work, these different configurations represent different perceptron weights, and we evaluate their similarity using the Hamming distance between the binary weights. In this setup, previous work [15] has obtained the phase diagram of the coupled perceptron problem for both the storage problem and the teacher-student scenario, but only at zero temperature.

In this paper, we focus exclusively on the teacher-student scenario, where the generalization error is quantified using the distance between the weights of the teacher and the student. To better understand the crucial role of different copycat students learning together, we introduce a crucial generalization of previous work by considering thermal noise. Namely, temperature allows students to make errors in classifying labels assigned by the teacher, and without such errors, learning cannot occur. The temperature parameter plays a crucial role in modeling the collective learning process as an annealing process, where temperature (and errors) decrease over time. In this context, we study the equilibrium properties of a model of coupled (copycat students) binary perceptrons in the *teacher-student* scenario and discuss how the phase diagram, and in particular the threshold for reaching perfect generalization solutions, changes when the system is replicated finitely many times (i.e., has a certain number y of students trying to learn the same rule with the same data) and explicit coupling between replicas γ is added. Our results show that having multiple coupled perceptrons learn in tandem reduces the amount of data required compared to individual learning. Moreover, this collaborative approach significantly accelerates the learning process compared to solo learning.

The structure of this paper is as follows: First, we introduce our coupled perceptron model and the associated learning rules. This is followed by an overview of the mean-field analytical approach we use to determine the free energy and subsequently, the phase diagram based on the ratio of examples reviewed by the students, α , and the temperature T . The Results section elaborates on this, including the influence of the number of replicas and their inter-coupling strength, especially investigated within a numerical simulated annealing framework. We conclude with a discussion and summary of our results.

II. MODEL

The model we consider is defined by a number y of binary perceptron students and a teacher perceptron. Each

student u is parameterized by a weight vector with N components $\mathbf{w}_u = \{w_{i,u}\}_{i=1}^N$ with $w_{i,u} \in \{-1, 1\}$, and $u \in \{1, \dots, y\}$, while we denote by \mathbf{w}_0 the teacher's weight. Students are given with the same set of M labeled data points, each represented by a pair $(\boldsymbol{\xi}^\mu, \sigma_0^\mu)$: the first is the training sample $\boldsymbol{\xi}^\mu$, an N -dimensional vector with binary entries $\xi_i^\mu \in \{-1, 1\}$, and σ_0^μ is the corresponding label, assigned by a teacher perceptron. We define the input-output ratio of the teacher and the students respectively as:

$$\sigma_0^\mu = \text{sign}(\omega_0^\mu) \quad \text{and} \quad \omega_0^\mu = \frac{\mathbf{w}_0 \cdot \boldsymbol{\xi}^\mu}{\sqrt{N}}, \quad (1)$$

$$\sigma_u^\mu = \text{sign}(\omega_u^\mu) \quad \text{and} \quad \omega_u^\mu = \frac{\mathbf{w}_u \cdot \boldsymbol{\xi}^\mu}{\sqrt{N}}, \quad (2)$$

for all $\mu \in \{1, \dots, M\}$, where the symbol \cdot denotes the scalar product. The normalization factor in Eq. (1) is chosen such that the energy of the model is extensive in the system size N . Each student adjusts their weights to minimize an appropriate cost function, which in general accounts for the number of misclassified examples, i.e., those for which their label differs from the teacher's prescription. Moreover, students interact through a pairwise ferromagnetic coupling, favoring configurations in which students have high mutual overlap; in other words, imitation between students is favored. At nonzero temperature, each student assigns a nonzero energetic cost to the misclassified data, i.e., if the student's output differs from the teacher's, $\sigma_u^\mu \neq \sigma_0^\mu$. We now need to define learning by specifying the actual Hamiltonian of the system. Following [30], we first define the *stability parameters* as

$$\Delta_u^\mu \triangleq \sigma_0^\mu \frac{\mathbf{w}_u \cdot \boldsymbol{\xi}^\mu}{\sqrt{N}}, \quad (3)$$

where $\Delta_u^\mu > 0$ whenever the input μ is correctly classified by the student u (i.e., as prescribed by the teacher). We can now define an arbitrary potential

$$V(\Delta) = (-\Delta)^\nu \Theta(-\Delta), \quad (4)$$

where $\Theta(x)$ denotes the Heaviside step function. Equation (4) assigns a 0 energy to the weight vectors that correctly classify a given pattern (i.e., those for which $\Delta > 0$) and adds a positive cost to misclassified data that is proportional to the stability of the misclassified data point to a power ν . The Hamiltonian of the model can therefore be written as follows:

$$\beta \mathcal{H}(\{\mathbf{w}_u\}_{u=1}^y \mid \mathbf{w}^0, \mathbb{D}) = \beta \sum_{u=1}^y \sum_{\mu=1}^M V(\Delta_u^\mu) - \frac{\gamma}{y} \sum_{u < v} \mathbf{w}_u \cdot \mathbf{w}_v \quad (5)$$

where $\mathbb{D} = \{\boldsymbol{S}^\mu\}_{\mu=1}^M$ denotes the full training set of teacher examples. The second term quantifies the interaction between students and is proportional to the Hamming distance between student weight pairs. Eq. (5) describes a system in which y students try to learn the

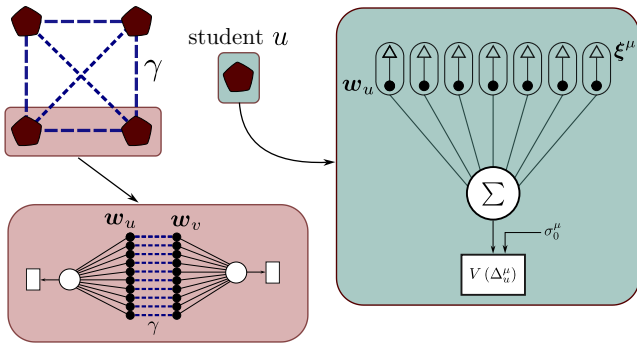


Figure 1. Schematic representation of the model defined by Eq. (5). For simplicity, we consider here $y = 4$ student perceptrons interacting over a fully connected graph, and the structure of each perceptron is shown in the green square. The dashed blue lines represent the coupling γ between students, proportional to the Hamming distance between the corresponding weight vectors \mathbf{w}_u and \mathbf{w}_v , as illustrated in the red square.

same rule given by a perceptron teacher while interacting with a ferromagnetic potential, the latter favoring configurations in which the students have a similar weight vector, i.e., when students are actively encouraged to be “inspired” by their peer perceptrons. We sketch the architecture of our coupled perceptron model in Fig. 1.

Different choices for the exponent ν define different dynamics, or learning rules, and lead to different properties of convergence and different phase diagrams in the thermodynamic limit [23, 31, 32]. In this article we will focus on the case $\nu = 1$, called the *perceptron rule*, originally introduced by Rosenblatt in Ref. [33] for the version with continuous weights. The case $\nu = 0$ is of no interest to us since the system remains frozen at all temperatures [31], and the case $\nu = 2$ is left for further studies.

In contrast to recent work in which a large deviation analysis is performed by considering the free energy as a function of the (normalized) Hamming distance between students [14, 16, 25], here we consider a scenario in which each student fluctuates with the heat bath at a given inverse temperature β and at fixed interaction strengths between students, γ , and we want to characterize whether and how the different operating regimes of the binary perceptron change when we consider multiple replicas of the same model with an explicit coupling. In other words, our goal is to understand and model how the collective or cooperative learning of multiple students differs at a fundamental level from that of a single student.

III. MEAN-FIELD THEORY

To characterize the equilibrium properties of the model (5), we need to compute the quenched free energy in the thermodynamic limit where both $N, M \rightarrow \infty$ with a finite ratio $\alpha = M/N$. The set of patterns $\{\xi^\mu\}_{\mu=1}^M$

and the teacher vector represent the sources of quenched disorder to be averaged over. Each student has access to the same amount of information, so that the disorder is the same for all students. The starting point of the derivation is the partition function

$$Z = \sum_{\mathbf{w}_u} \exp \left[-\beta \sum_{u,\mu} V(\Delta_u^\mu) + \frac{\gamma}{y} \sum_{u < v} \mathbf{w}_u \cdot \mathbf{w}_v \right], \quad (6)$$

where we consider that the thermal noise only affects the first term in the Hamiltonian, but not the coupling between the students: this choice allows for a finite coupling γ between replicas even in the 0- temperature limit, where the model is reduced to a CSP in the space of student weights satisfying the constraints imposed by the teacher. This is also the same model analyzed at $T = 0$ in several recent works [14–16, 25].

The final object to be computed is the quenched free energy density

$$\mathcal{G}(\alpha, \beta, \gamma, y) = \lim_{N \rightarrow \infty} \frac{1}{Ny} \langle \log Z \rangle_{\mathbb{D}, \mathbf{w}^0}. \quad (7)$$

For simplicity, we restrict ourselves to finite values of y , although in principle the limit $y \rightarrow \infty$ could also be analyzed, since the coupling between the students is rescaled so that (7) is an intensive quantity with respect to both N and y . The computation of (7) can be performed as usual in spin-glass theory using the replica trick [34, 35]. The additional problem here lies in the coupled students, which formally play the same role as “real” replicas, since they share the same quenched disorder, the only difference being their explicit pairwise coupling. The calculations (explained in detail in Appendix A) require the introduction of a set of order parameters for the theory to be evaluated by the saddle point method in the thermodynamic limit: Namely, the order parameters are the overlap with the teacher vector for each student (in each replica)

$$R_a^u = \frac{1}{N} \sum_i w_{i,u}^{(a)} w_i^0, \quad (8)$$

and the two-replica overlap between two students u, v :

$$q_{ab}^{uv} = \frac{1}{N} \sum_i w_{i,u}^{(a)} w_{i,v}^{(b)}. \quad (9)$$

It is perhaps more instructive to visualize the overlaps (9) in a block-matrix form. We can indeed write a $n \times n$ block matrix of the type

$$\mathcal{Q} = \begin{bmatrix} \mathcal{Q}_{11} & \cdots & \mathcal{Q}_{1n} \\ \vdots & \ddots & \vdots \\ \mathcal{Q}_{n1} & \cdots & \mathcal{Q}_{nn} \end{bmatrix} \quad (10)$$

where each inner matrix \mathcal{Q}_{ab} has dimension $y \times y$. Each of these matrices describes the typical 2-point overlap between students with two generic replica indices a and

b. The simplest ansatz that can be implemented, imposes a symmetry between the order parameters in the replica space. This would be equivalent to assuming that

$$(\mathcal{Q}_{ab})_{uv} = q_{ab}^{uv} = q \quad \forall a \neq b \quad (11)$$

for the off-diagonal blocks of (10). On the other hand, the diagonal blocks represent the average correlation between the students, which in general may depend on the topology of the interactions in the starting Hamiltonian. However, assuming a fully-connected topology of interactions as in (5), it is natural to assume a uniform overlap between students $u \neq v$ in the *same* replica a , namely

$$(\mathcal{Q}_{aa})_{uv} = q_{aa}^{uv} = \delta_{uv} + p(1 - \delta_{uv}) \quad \forall a, \quad (12)$$

where the diagonal term δ_{uv} comes from the binary nature of the weights. Due to the different nature of the replicas a, b and students u, v , the two values of the overlap used in this ansatz are expected to be different, and in particular, $p \geq q$ due to the ferromagnetic coupling γ in the Hamiltonian (with the equality holding at $\gamma = 0$). The signal term R_a^u describing the average coupling with the teacher vector, a replica symmetric ansatz on both replica spaces will imply

$$R_a^u = R \quad \forall u, a. \quad (13)$$

The final quenched free energy (7) can be written as

$$\mathcal{G} = -R\hat{R} - \frac{(y-1)}{2}p\hat{p} + \frac{\hat{q}}{2}(yq-1) + \alpha G_E(R, q, p, \beta) + G_I(\hat{R}, \hat{p}, \hat{q}, \gamma). \quad (14)$$

Interestingly, the entropic term G_I in the free energy can be viewed as an averaged log-partition function of a reduced system of y degrees of freedom (in this case binary spins as the original weights), which is subject to an effective coupling whose strength depends both on the overlaps and on the explicit replica-coupling γ , plus a random Gaussian field over which must be averaged.

IV. RESULTS

Fig. 2 shows the phase diagram of the model under the Replica Symmetric ansatz, with a further symmetry assumption between the students. We begin by discussing the standard phase diagram of the (single) perceptron, equipped with the rule (4) and $\nu = 1$, shown in Fig. 2–above. This phase diagram was previously obtained by Horner in 1992 [31]. For $0.05 \lesssim T \lesssim 0.2$, three different equilibrium regimes can be distinguished by increasing the number of examples reviewed by the student α : before the dashed line (in region (a)), the free energy has a unique minimum corresponding to a solution with $R < 1$, i.e. an imperfect generalization, (recall that R is the averaged overlap between the student and the teacher, i.e. the planted configuration to be found); to the right of

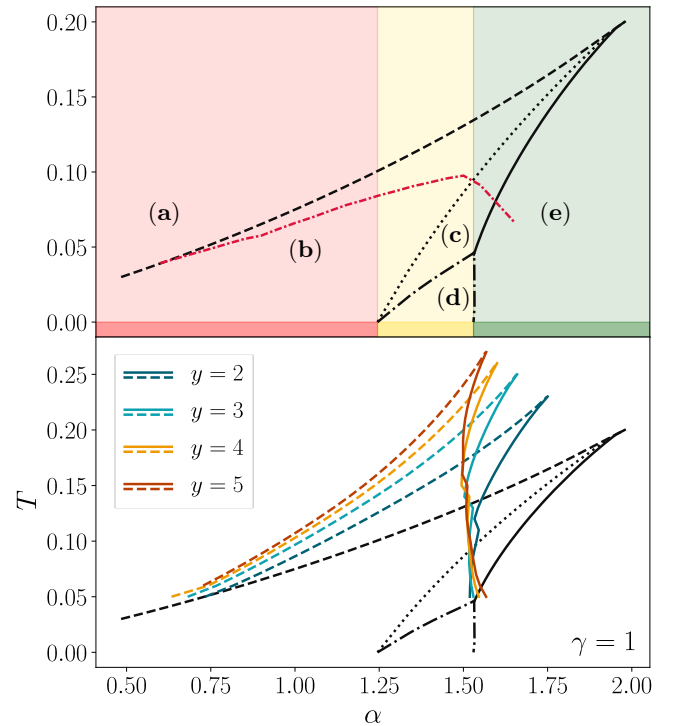


Figure 2. Equilibrium phase diagram of binary perceptron equipped with the Perceptron rule (4). **Top panel:** Phase diagram of the non-replicated system. In (a), all free energy minima correspond exclusively to configurations with non-zero generalization error ε_g , i.e. $R \ll 1$. In (b) There exists a minimum with $R \approx 1$, but it is subdominant; ground states have $\varepsilon_g \neq 0$ for $\alpha < 1.245$. This is the *impossible* inference phase (pink area). In (c) the zero-generalization ($\varepsilon_g = 0$ and $R = 1$) minimum becomes dominant in the free energy. In (d) spin-glass phase where replica symmetric entropy becomes negative, broken replica symmetry ansatz required. At $T = 0$ unique ground state corresponding to the teacher but *hard* inference phase (yellow region). In (e) the teacher solution is the only minimum, all other solutions vanish. This is the *easy* phase (in green). Below the dashed red line, non-generalizing glassy states begin to appear. These solutions are the 1RSB solutions (with Parisi’s $m = 1$ parameter), thus indicating the presence of a dynamic phase transition. In **bottom panel**, comparison with the corresponding replicated phase diagrams obtained with fixed coupling $\gamma = 1$ for different values of y (indicated in the legend).

it, (i.e. at (b)), the teacher’s solution appears, with $R = 1$, but it is metastable (subdominant). As soon as the dashed line is crossed, the teacher’s solution becomes thermodynamically dominant (in the region (c)) and finally the imperfect generalization minimum of free energy disappears after the solid line (region (e)), where any other solution with imperfect generalization ($R < 1$) disappears at the RS level. The region (d) corresponds to the spin-glass phase, i.e. $R < 1$ and q and p high, which is discovered in practice because the replica symmetric entropy becomes negative – a clear sign that the replica symmetry ansatz is no longer valid, or can be found using

the one-step replica symmetry breaking ansatz (1-RSB). Finally, we can also identify the onset in temperature where poor generalization of glassy states ($R < 1$, $p = 1$ and q high) becomes metastable but subdominant (below the dense dashed red lines), which can be seen as a proxy of the dynamical transition line and can be found using the 1RSB ansatz looking for solutions with $p \sim 1$. There are in principle other transitions at low temperatures, as discussed in [31], but they are not useful for our purposes here.

Theoretically, this means that for a given α one can infer the performance of a simulated annealing experiment (or a learning process modelled by a slow decrease of the allowed number of errors allowed) based on this mean field phase diagram. If $\alpha \gtrsim 1.52$, it should be possible in practice to find the ground state (i.e., the teacher weights) using SA, since the non-perfect solution vanishes at a low enough temperature. At the temperature where the non-perfect solution vanishes and in absence of other states, the system will melt into the teacher's state. For a smaller value of α it is not possible either because the SA would be trapped in the non-perfect solution and eventually end up in a spin-glass phase, or because the teacher's solution is as good as exponentially many others. This leads to the conclusion that the higher $\alpha > 1.52$ is, the easier it should be to find the teacher, since the free energy landscape is smoother. However, as shown in Fig. 3, it is in practice very difficult to find the ground state using the SA method for $\alpha = 1.6$ with $y = 1$ (no replica).

In 2-bottom, we show instead how the phase diagram shifts when there is a nonzero replica coupling γ , as a function of the number of students involved. Fig. 2-bottom illustrates how the spinodal lines change when y coupled replicas are introduced. The most interesting phenomenon is that the upper right part of the spinodal seems to push toward lower values of α . In other words, when performing SA the perceptron will not encounter the poorly generalizing state, or, this state would have melt much before. In practice, this phase diagram shows us that many coupled students need to go through fewer data examples to perfectly deduce the teacher's rule.

Moreover, the location of the regions where metastable states with poor generalization occur also allows us to draw conclusions about whether or not a SA strategy can succeed in learning the correct teacher rules, but also whether or not learning can be done fast.

A. Simulated Annealing

In this section, we investigate numerically the effects of shifting the critical lines in the phase diagram when adding replicas and for different values of the cooling rate. First, the Simulated Annealing protocol corresponds to performing a number of n Monte Carlo sweeps (an update of the entire system in random order) before reducing the temperature as $\Delta T = -\eta$. Fig 3 shows the generalization error as a function of the temperature by running

numerical SA experiments SA on the model with y many replicas for three different values of α with a cooling rate of $\eta = 10^{-5}$. We see that even in cases where it should be easy to find the teacher's solution, as for instance the case $y = 1$ at $\alpha = 1.5$, (that lays in the region where a perfect generalisation is the ground state) it is very difficult to find the right solutions. However, when $y > 1$, we manage to obtain the teacher's configuration even in domains the sub-optimal solution should have been obtained $\alpha \lesssim 1.5$. Looking at the phase diagram, we see that it is possible to track the teacher's state up to $\alpha 1.5$ without crossing sub-optimal solution as we add more and more replicas. The SG phase, where a lower temperature prevails, would not be a problem in this case, since the system would be trapped in the teacher's state before reaching the SG phase. To the contrary, when for system without replica, $y = 1$, approaches the values of $\alpha < 1.6$, the system may not melt from the non-generalizing state to the teacher state due to the occurrence of subdominant spin-glass states. In Fig. 4 we show the success probability of a SA for different numbers of replicas, cooling rate, and values of α (each point is averaged over 50 seeds). Our experiments strongly suggest that the free energy landscape is smoothed when coupled replicas are added to the system. The systems with many replicas can avoid melting into subdominant SG states and therefore make it easier for SA to find the ground state of the system. More details on the calculations can be found in the Appendix B.

V. DISCUSSION

In this paper, we have illustrated how the phase diagram of the perceptron in the teacher-student scenario changes as more and more perceptron-students coupled together are added to the equation. Using this phase diagram, we can draw conclusions not only about the number of examples required for perfect generation as a function of the number of students working together, which is much lower than for a single perceptron, but also about the performance of a learning process modeled as a simulated annealing process in which the goal is to derive the teacher's rule while gradually lowering the temperature, which, by analogy, minimizes the student's allowable errors.

The coupled perceptron model discussed here provides a basic model for understanding the effectiveness of students' collective learning in acquiring a particular set of pre-established rules. Alternatively, our model could also be used to rationalise the effects of federated or collaborative learning in Machine Learning, a decentralized approach to training models. In both contexts, our phase diagrams facilitate the determination of the ideal number of collaborating teams, the best number of examples, or the most appropriate pace of learning to ensure optimal learning outcomes. Within the context of this rudimentary model, further generalisations could address the

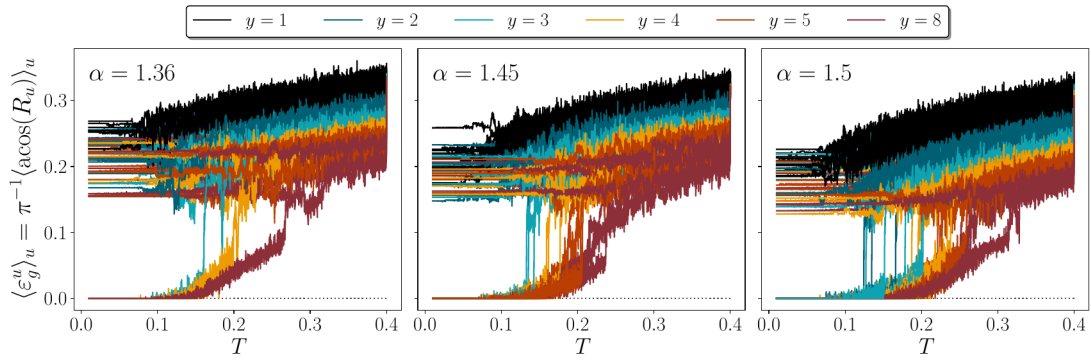


Figure 3. Numerical training trajectories obtained by running a Simulated Annealing algorithm in models having different number of coupled replicas. Here we show the generalization error for systems of size $N = 1001$ and $\alpha = 1.36, 1.45$ and 1.5 . We see that even in the case where it should be impossible to find solutions for a single perceptron ($\alpha \lesssim 1.52$), the replicated model manages to converge easily to the teacher configuration.

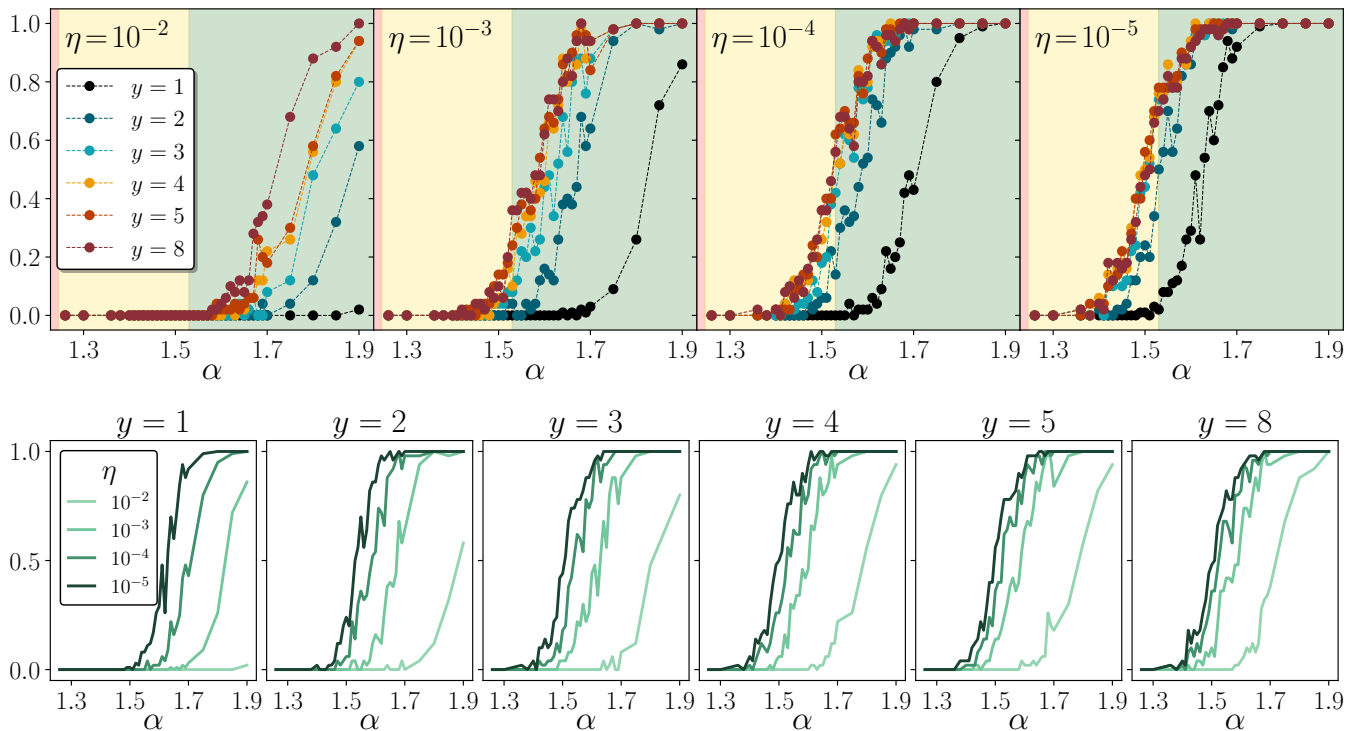


Figure 4. **Top panel:** we show the success probability (calculated over 50 seeds) that the system finds the right teacher solution through a Simulated Annealing process, for different values of α , with $N = 1001$ weights. From left to right, different cooling rates η . We clearly see the advantage of the coupled replicas. At the lowest cooling rate, the case with $y = 8$ replicas manages to find a solution in the hard inference region with probability ~ 0.8 . **Bottom panel:** same plots but ordered by the value of y , where we can clearly observe that the cooling rate seems to converge to the same curves in the case $y = 5$ and 8 .

question of whether diversifying examples for each student improves the learning experience or whether alternative learning paths could accelerate the learning process.

From a technical point of view, we believe that this work contributes to a better understanding of the role of the robust ensemble, which has recently been proposed to design novel algorithmic schemes to find solutions of constraint-satisfaction problems (but not only

those). Specifically, the non-perfect generalization solution with $R < 1$ ceases to exist at *smaller* values of α , so less data is required to learn the same rule perfectly (at least in this very simplified model). Although the left-to-right motion in the phase diagrams of Fig. 2 is typically a non-realistic situation in full batch learning, it could play an important role in an online learning scenario and provide insight into the expected outcome of algorithms

for local search. Our results suggest that coupled neural networks can, in principle, perform better in terms of generalization error for a fixed amount of data. It would be interesting to verify this effect for more complex architectures in a supervised learning task. In a continuous version, an equivalent analysis can be performed. In this case, we simply expect a decrease in the generalization error at fixed α , as it is always an asymptotically decreasing function of α with no transition.

Finally, we note that the twist of the phase diagram at the boundary between the hard and easy (for equilibrium theory) regions of the phase diagram suggests that the nature of the phase transition could change to a second order phase transition for a small interval of $\alpha < 1.52$; this would be in perfect agreement with the results of [18] and could in principle be studied in the limit $y \rightarrow \infty$.

ACKNOWLEDGMENTS

We thank Federico Ricci-Tersenghi and Carlo Lucibello for useful discussions and suggestions regarding this article. All the authors acknowledge financial support by the Comunidad de Madrid and the Complutense University of Madrid (UCM) through the Atracción de Talento programs (Refs. 2019-T1/TIC-13298 and 2019-T1/TIC-12776), the Banco Santander and the UCM (grant PR44/21-29937), and Ministerio de Economía y Competitividad, Agencia Estatal de Investigación and Fondo Europeo de Desarrollo Regional (Ref. PID2021-125506NA-I00). B.S. acknowledges the support of the Agence Nationale de la Recherche (Ref. ANR CPJ-ESE 2022).

-
- [1] L. Zdeborová and F. Krzakala, *Advances in Physics* **65**, 453 (2016).
- [2] S. S. Mannelli, G. Biroli, C. Cammarota, F. Krzakala, P. Urbani, and L. Zdeborová, *Physical Review X* **10**, 011057 (2020).
- [3] M. Mézard, G. Parisi, and R. Zecchina, *Science* **297**, 812 (2002).
- [4] L. Zdeborová and F. Krzakala, *Physical Review E* **76**, 031131 (2007).
- [5] F. Krzakala and L. Zdeborová, *Physical review letters* **102**, 238701 (2009).
- [6] E. Gardner and B. Derrida, *Journal of Physics A: Mathematical and general* **21**, 271 (1988).
- [7] W. Krauth, M. Mézard, and J.-P. Nadal, *Complex Systems* **2**, 387 (1988).
- [8] R. Monasson and R. Zecchina, *Physical review letters* **75**, 2432 (1995).
- [9] R. Monasson and R. Zecchina, *Modern Physics Letters B* **9**, 1887 (1995).
- [10] R. Dietrich, M. Opper, and H. Sompolinsky, *Phys. Rev. Lett.* **82**, 2975 (1999).
- [11] E. Barkai, D. Hansel, and H. Sompolinsky, *Phys. Rev. A* **45**, 4146 (1992).
- [12] E. Cornacchia, F. Mignacco, R. Veiga, C. Gerbelot, B. Loureiro, and L. Zdeborová, *Machine Learning: Science and Technology* **4**, 015019 (2023).
- [13] S. Franz and G. Parisi, *Journal of Physics A: Mathematical and Theoretical* **49**, 145001 (2016).
- [14] C. Baldassi, A. Ingrosso, C. Lucibello, L. Saglietti, and R. Zecchina, *Journal of Statistical Mechanics: Theory and Experiment* **2016**, 023301 (2016), publisher: IOP Publishing and SISSA.
- [15] C. Baldassi, A. Ingrosso, C. Lucibello, L. Saglietti, and R. Zecchina, *Physical Review Letters* **115**, 128101 (2015), publisher: American Physical Society.
- [16] C. Baldassi, C. Borgs, J. T. Chayes, A. Ingrosso, C. Lucibello, L. Saglietti, and R. Zecchina, *Proceedings of the National Academy of Sciences* **113**, E7655 (2016), publisher: Proceedings of the National Academy of Sciences.
- [17] H. Huang, K. Y. M. Wong, and Y. Kabashima, *Journal of Physics A: Mathematical and Theoretical* **46**, 375002 (2013), publisher: IOP Publishing.
- [18] M. C. Angelini and F. Ricci-Tersenghi, *Physical Review X* **13**, 021011 (2023), publisher: American Physical Society.
- [19] W. Barthel, A. K. Hartmann, M. Leone, F. Ricci-Tersenghi, M. Weigt, and R. Zecchina, *Physical review letters* **88**, 188701 (2002).
- [20] W. Krauth and M. Mézard, *J. Phys.* **50**, 3057 (1989).
- [21] B. Aubin, W. Perkins, and L. Zdeborová, *Journal of Physics A: Mathematical and Theoretical* **52**, 294003 (2019).
- [22] G. Györgyi, *Phys. Rev. A* **41**, 7097 (1990).
- [23] H. S. Seung, H. Sompolinsky, and N. Tishby, *Phys. Rev. A* **45**, 6056 (1992).
- [24] T. L. H. Watkin, A. Rau, and M. Biehl, *Rev. Mod. Phys.* **65**, 499 (1993).
- [25] H. Huang and Y. Kabashima, *Phys. Rev. E* **90**, 10.1103/PhysRevE.90.052813 (2014).
- [26] R. Monasson, *Physical review letters* **75**, 2847 (1995).
- [27] S. Franz and G. Parisi, *Journal de Physique I* **5**, 1401 (1995).
- [28] M. Sellitto and F. Zamponi, *Europhysics Letters* **103**, 46005 (2013).
- [29] L. Berthier, P. Charbonneau, D. Coslovich, A. Ninarello, M. Ozawa, and S. Yaida, *Proceedings of the National Academy of Sciences* **114**, 11356 (2017).
- [30] A. Engel and C. Van den Broeck, *Statistical Mechanics of Learning* (Cambridge University Press, Cambridge, 2001).
- [31] H. Horner, *Zeitschrift für Physik B Condensed Matter* **87**, 371 (1992).
- [32] H. Horner, *Zeitschrift für Physik B Condensed Matter* **86**, 291 (1992).
- [33] F. Rosenblatt, *Psychological Review* **65**, 386 (1958).
- [34] M. Mezard, G. Parisi, and M. Virasoro, *Spin Glass Theory and Beyond* (WORLD SCIENTIFIC, 1986) <https://www.worldscientific.com/doi/pdf/10.1142/0271>.
- [35] P. Charbonneau, E. Marinari, G. Parisi, F. Ricci-Tersenghi, G. Sicuro, and F. Zamponi, *Spin glass theory and far beyond—replica symmetry breaking after 40 years* (2023).

Appendix A: Derivation of Quenched Free energy

In this section we discuss how to compute the averaged quenched free energy for the model (5). As standard in spin-glass models with some quenched disorder, the first step requires the introduction of a number n of replicas, whose limit $n \rightarrow 0$ is taken afterwards. These replicas differ from the one in the original model because they are independent and no explicit coupling is present between them. In the following derivation, and in order to avoid confusion between the two sets of replicas, we always use indices $a, b \in \{1, \dots, n\}$ to denote “fake” replicas and $u, v \in \{1, \dots, y\}$ to index students (i.e. real replicas in the original Hamiltonian). Replicating all the degrees of freedom $w_{i,u}$ n times (with n integer) we can write the replicated partition function as

$$Z^n = \sum_{\mathbf{w}_u^{(a)}} \exp \left[-\beta \sum_{a,u,\mu} V(\Delta_{u,a}^\mu) + \frac{\gamma}{y} \sum_a \sum_{u < v} \mathbf{w}_u^{(a)} \cdot \mathbf{w}_v^{(a)} \right]. \quad (\text{A1})$$

We start by introducing the definition of the stabilities

$$\Delta_{u,a}^\mu = \sigma_0^\mu \frac{\mathbf{w}_u^{(a)} \cdot \boldsymbol{\xi}^\mu}{\sqrt{N}}, \quad (\text{A2})$$

with σ_0^μ given by Eq. (1) in the main text. Enforcing definitions (A2) and (1) by using delta functions and exploiting their Fourier representation, the partition function (A1) can be re-written as

$$\begin{aligned} Z^n = & \sum_{\mathbf{w}_u^{(a)}} \int \prod_{\mu} d\omega_0^\mu d\hat{\omega}_0^\mu \int \prod_{\mu,a,u} d\Delta_{u,a}^\mu d\hat{\Delta}_{u,a}^\mu \exp \left[-\beta \sum_{a,u,\mu} V(\Delta_{u,a}^\mu) + \frac{\gamma}{y} \sum_a \sum_{u < v} \mathbf{w}_u^{(a)} \cdot \mathbf{w}_v^{(a)} \right] \\ & \times \exp \left[i \sum_{\mu} \omega_0^\mu \hat{\omega}_0^\mu - \frac{i}{\sqrt{N}} \sum_{\mu} \hat{\omega}_0^\mu (\mathbf{w}^0 \cdot \boldsymbol{\xi}^\mu) + i \sum_{a,\mu,u} \Delta_{u,a}^\mu \hat{\Delta}_{u,a}^\mu - \frac{i}{\sqrt{N}} \sum_{a,\mu,u} \hat{\Delta}_{u,a}^\mu \sigma_0^\mu (\mathbf{w}_u^{(a)} \cdot \boldsymbol{\xi}^\mu) \right]. \quad (\text{A3}) \end{aligned}$$

where $\hat{\omega}_0^\mu$ (resp. $\hat{\Delta}_{u,a}^\mu$) are the conjugate variables of ω_0^μ (resp. $\Delta_{u,a}^\mu$) introduced through a Fourier transform. It is now easy to perform the average over the disorder given by the pattern components. As specified in the main text, we assume them to be i.i.d. with binary components, so that $\xi_i^\mu \in \{-1, 1\}$ with equal probability. As for now we do not perform the average over the teacher weight vector, but anyways it will become trivial in the final expression. The average concerns only the second and fourth term in the second line of (A3):

$$\begin{aligned} \left\langle e^{-\frac{i}{\sqrt{N}} \sum_{\mu} \hat{\omega}_0^\mu (\mathbf{w}^0 \cdot \boldsymbol{\xi}^\mu) - \frac{i}{\sqrt{N}} \sum_{a,\mu,u} \hat{\Delta}_{u,a}^\mu \sigma_0^\mu (\mathbf{w}_u^{(a)} \cdot \boldsymbol{\xi}^\mu)} \right\rangle_{\{\xi^\mu\}_{\mu=1}^M} &= \prod_{i,\mu} \left\langle \exp \left[-\frac{i}{\sqrt{N}} \xi_i^\mu \left(\hat{\omega}_0^\mu w_i^0 + \sigma_0^\mu \sum_{a,u} \hat{\Delta}_{u,a}^\mu w_{i,u}^{(a)} \right) \right] \right\rangle_{\xi_i^\mu} \\ &= \prod_{i,\mu} 2 \cosh \left[\frac{i}{\sqrt{N}} \left(\hat{\omega}_0^\mu w_i^0 + \sigma_0^\mu \sum_{a,u} \hat{\Delta}_{u,a}^\mu w_{i,u}^{(a)} \right) \right] \\ &\approx \exp \left[-\frac{1}{2N} \sum_{i\mu} \left(\hat{\omega}_0^\mu w_i^0 + \sigma_0^\mu \sum_{a,u} \hat{\Delta}_{u,a}^\mu w_{i,u}^{(a)} \right)^2 \right], \quad (\text{A4}) \end{aligned}$$

where in the first line we use the fact that pattern components are i.i.d. and in the last line we expanded for $N \rightarrow \infty$, keeping only the first order, the other ones being subdominant in the thermodynamic limit. Let us first rearrange a bit the square term in the above expression as

$$\begin{aligned} \left(\hat{\omega}_0^\mu w_i^0 + \sigma_0^\mu \sum_{a,u} \hat{\Delta}_{u,a}^\mu w_{i,u}^{(a)} \right)^2 &= (\hat{\omega}_0^\mu)^2 + 2\hat{\omega}_0^\mu \sigma_0^\mu w_i^0 \sum_{a,u} \hat{\Delta}_{u,a}^\mu w_{i,u}^{(a)} + \sum_{a,u} (\hat{\Delta}_{u,a}^\mu)^2 + \\ &+ 2 \sum_a \sum_{u < v} \hat{\Delta}_{u,a}^\mu \hat{\Delta}_{v,a}^\mu w_{i,u}^{(a)} w_{i,v}^{(a)} + 2 \sum_{a < b} \sum_{u,v} \hat{\Delta}_{u,a}^\mu \hat{\Delta}_{v,b}^\mu w_{i,u}^{(a)} w_{i,v}^{(b)}. \quad (\text{A5}) \end{aligned}$$

As usual, the disorder average results into an effective coupling between replicas a, b , and another coupling will also be taken into account between students in the same replica a on top of the explicit one in the Hamiltonian. We can

now introduce a set of order parameters, namely the overlap between student u (in replica a) with the teacher and the two-replica overlap between two student vectors u, v , respectively given by:

$$R_a^u = \frac{1}{N} \sum_i w_{i,u}^{(a)} w_i^0 \quad (\text{A6})$$

$$q_{ab}^{uv} = \frac{1}{N} \sum_i w_{i,u}^{(a)} w_{i,v}^{(b)} \quad (\text{A7})$$

As discussed in the main text, it is easy to visualize (A7) in terms of a $ny \times ny$ matrix with a block structure made of n blocks of size y along each dimension. Exploiting trivial symmetries under index permutations, the number of independent overlaps turns out to be equal to $n \binom{y}{2} + \binom{n}{2} y^2 = \binom{ny}{2}$. Enforcing definitions (A6)-(A7) through delta functions and substituting (A5) into the partition function, we can rewrite it as

$$\begin{aligned} \langle Z^n \rangle_{\mathcal{D}} = \sum_{\mathbf{w}_u^{(a)}} \int \prod_{a,u} dR_a^u d\hat{R}_a^u \int \prod_{a,b,u,v \in \mathcal{P}} dq_{ab} d\hat{q}_{ab} \int \prod_{\mu} d\omega_0^\mu d\hat{\omega}_0^\mu \int \prod_{\mu,a,u} d\Delta_{u,a}^\mu d\hat{\Delta}_{u,a}^\mu \exp \left[-\beta \sum_{a,u,\mu} V(\Delta_{u,a}^\mu) + \right. \\ \left. + i \sum_{\mu} \omega_0^\mu \hat{\omega}_0^\mu + i \sum_{a,\mu,u} \Delta_{u,a}^\mu \hat{\Delta}_{u,a}^\mu + iN \sum_{a,u} R_a^u \hat{R}_a^u + iN \sum_{a,b,u,v \in \mathcal{P}} q_{ab}^{uv} \hat{q}_{ab}^{uv} - \frac{1}{2} \sum_{\mu} (\hat{\omega}_0^\mu)^2 \right. \\ \left. - \sum_{\mu} \hat{\omega}_0^\mu \sigma_0^\mu \sum_{a,u} \hat{\Delta}_{u,a}^\mu R_a^u - \frac{1}{2} \sum_{\mu,a,u} (\hat{\Delta}_{u,a}^\mu)^2 - \sum_{\mu,a} \sum_{u < v} q_{aa}^{uv} \hat{\Delta}_{u,a}^\mu \hat{\Delta}_{v,a}^\mu - \sum_{\mu} \sum_{a < b} \sum_{u,v} q_{ab}^{uv} \hat{\Delta}_{u,a}^\mu \hat{\Delta}_{v,b}^\mu + \right. \\ \left. + \frac{\gamma}{y} \sum_a \sum_{u < v} \mathbf{w}_u^{(a)} \cdot \mathbf{w}_v^{(a)} - i \sum_{a,u} \hat{R}_a^u \sum_i w_{i,u}^{(a)} w_i^0 - i \sum_{a,b,u,v \in \mathcal{P}} \hat{q}_{ab}^{uv} \sum_i w_{i,u}^{(a)} w_{i,v}^{(b)} \right] \quad (\text{A8}) \end{aligned}$$

where the symbol \mathcal{P} is a short-hand notation to indicate all the possible independent overlaps, specifically $\sum_{a,b,u,v \in \mathcal{P}} = \sum_a \sum_{u < v} + \sum_{a < b} \sum_{u,v}$. We can notice now how the integrals over μ -dependent quantities can be factorized, as well as the sum over weight components i . We can therefore rewrite Eq. (A8) in a saddle point form. Using the property that the teacher vector components are i.i.d., we can write

$$\langle Z^n \rangle_{\mathcal{D}, \mathbf{w}_0} = \int \prod_{a,u} dR_a^u d\hat{R}_a^u \int \prod_{a,b,u,v \in \mathcal{P}} dq_{ab} d\hat{q}_{ab} \exp \left[Ny \mathcal{G} \left(\left\{ R_a^u, q_{ab}^{uv}, \hat{R}_a^u, \hat{q}_{ab}^{uv} \right\} \right) \right] \quad (\text{A9})$$

$$\mathcal{G} \left(\left\{ R_a^u, q_{ab}^{uv}, \hat{R}_a^u, \hat{q}_{ab}^{uv} \right\} \right) = \frac{i}{y} \sum_{a,u} R_a^u \hat{R}_a^u + \frac{i}{y} \sum_{a,b,u,v \in \mathcal{P}} q_{ab}^{uv} \hat{q}_{ab}^{uv} + \frac{\alpha}{y} G_E \left(\left\{ R_a^u, q_{ab}^{uv} \right\} \right) + \frac{1}{y} G_I \left(\left\{ \hat{R}_a^u, \hat{q}_{ab}^{uv} \right\} \right) \quad (\text{A10})$$

where \mathcal{G} plays the role of a free energy with opposite sign. The equilibrium behavior is thus determined by the maximum of \mathcal{G} w.r.t. the order parameters. The quantities G_E and G_I represent the usual entropic and energetic terms, respectively given by

$$G_I = \mathbb{E}_{\mathbf{w}_0} \log \sum_{w_u^a \in \{-1,1\}} \exp \left[\frac{\gamma}{y} \sum_a \sum_{u < v} w_u^a w_v^a - i w_0^0 \sum_{a,u} \hat{R}_a^u w_u^a - i \sum_{a,b,u,v \in \mathcal{P}} \hat{q}_{ab}^{uv} w_u^a w_v^b \right] \quad (\text{A11})$$

$$\begin{aligned} G_E = \log \int d\omega_0 d\hat{\omega}_0 d\Delta_u^a d\hat{\Delta}_u^a \exp \left[-\beta \sum_{a,u} V(\Delta_u^a) + i\omega_0 \hat{\omega}_0 + i \sum_{a,u} \Delta_u^a \hat{\Delta}_u^a - \frac{1}{2} \hat{\omega}_0^2 - \frac{1}{2} \sum_{a,u} (\hat{\Delta}_{u,a}^a)^2 + \right. \\ \left. + \hat{\omega}_0 \sigma_0 \sum_{a,u} \hat{\Delta}_u^a R_a^u - \frac{1}{2} \sum_{a,u \neq v} \hat{\Delta}_u^a \hat{\Delta}_v^a q_{aa}^{uv} - \frac{1}{2} \sum_{a \neq b} \sum_{u,v} \hat{\Delta}_u^a \hat{\Delta}_v^b q_{ab}^{uv} \right] \quad (\text{A12}) \end{aligned}$$

where in the last line we exploited the fact that the teacher vector components are i.i.d. by assumption, and the resulting expectation over one representative component w_0 is now dummy by means of a gauge transformation $\sigma_u^a \rightarrow w_0^0 \sigma_u^a$ for all the spin components. Before going on, note that the integral over $\hat{\omega}_0$ in Eq. (A12) can be carried out explicitly, leading to

$$G_E = \log \int \mathcal{D}\omega_0 d\hat{\omega}_0 d\Delta_u^a d\hat{\Delta}_u^a \exp \left\{ -\beta \sum_{a,u} V(\Delta_u^a) + i \sum_{a,u} \hat{\Delta}_u^a (\Delta_u^a - \omega_0 \sigma_0 R_a^u) - \frac{1}{2} \sum_{a,u} [1 - (R_a^u)^2] (\hat{\Delta}_{u,a}^u)^2 \right. \\ \left. - \frac{1}{2} \sum_{a,u \neq v} \hat{\Delta}_u^a \hat{\Delta}_v^a (q_{aa}^{uv} - R_a^u R_a^v) - \frac{1}{2} \sum_{a \neq b} \sum_{u,v} \hat{\Delta}_u^a \hat{\Delta}_v^b (q_{ab}^{uv} - R_a^u R_b^v) \right\} \quad (\text{A13})$$

where $\mathcal{D}x = e^{-x^2/2} dx / \sqrt{2\pi}$ denotes the standard Gaussian probability measure.

1. Replica symmetric ansatz on both spaces

This corresponds to impose the following equations. For each ansatz we just write the final form of the free energy and the saddle point equations, when we decide which it works and which to put I can write some calculations, otherwise it's too long

$$R_a^u = R \quad \forall u, a \quad q_{aa}^{uv} = p \quad \forall u \neq v, a \quad q_{ab}^{uv} = q \quad \forall u, v, a \neq b \quad (\text{A14a})$$

$$\hat{R}_a^u = i\hat{R} \quad \forall u, a \quad \hat{q}_{aa}^{uv} = i\hat{p} \quad \forall u \neq v, a \quad \hat{q}_{ab}^{uv} = i\hat{q} \quad \forall u, v, a \neq b \quad (\text{A14b})$$

We have

$$G_I = -\frac{ny}{2} \hat{q} + n \mathbb{E}_{w^0} \int \mathcal{D}z \log \mathcal{Z}_{(y)}(\hat{R}, \hat{p}, \hat{q}, \gamma) \quad (\text{A15})$$

$$\mathcal{Z}_{(y)}(\hat{R}, \hat{p}, \hat{q}, \gamma) = \sum_{w_u \in \pm 1} \exp \left[\left(\frac{\gamma}{y} + \hat{p} - \hat{q} \right) \sum_{u < v} w_u w_v + (w^0 \hat{R} + \sqrt{\hat{q}} z) \sum_u w_u \right] \quad (\text{A16})$$

Interestingly, the entropic term can be seen as an averaged free energy (apart on a sign) of a reduced system of y degrees of freedom (in this case, binary spins due to the binary nature of the starting perceptron), with an effective ferromagnetic coupling, immersed in an external field given by the sum of two terms: a signal one proportional to \hat{R} , and a random Gaussian field z to be further averaged over. In the limit $n \rightarrow 0$, the free energy can be written as

$$\mathcal{G} = -R\hat{R} - \frac{(y-1)}{2} p\hat{p} + \frac{\hat{q}}{2} (yq - 1) + \frac{2\alpha}{y} \int \mathcal{D}t \Phi(at) \log \int \mathcal{D}\tau \Xi^y + \frac{1}{y} \int \mathcal{D}z \log \mathcal{Z}_{(y)}(\hat{R}, \hat{p}, \hat{q}, \gamma) \quad (\text{A17})$$

$$\Xi = \int \frac{d\Delta}{\sqrt{1-p}} \exp \left[-\beta V(\Delta) - \frac{1}{2(1-p)} (\Delta + \sqrt{qt} + \sqrt{p-q}\tau)^2 \right] \quad (\text{A18})$$

Explicit formulas for Ξ depend on the specific choice for the potential. Two examples are given below, respectively for the Gibbs and Perceptron learning rules :

$$V(\Delta) = \theta(-\Delta) \quad \longrightarrow \quad \Xi = \Phi(bt + c\tau) + e^{-\beta} \Phi\left(\beta\sqrt{1-p} - bt - c\tau\right) \quad (\text{A19})$$

$$V(\Delta) = -\Delta\theta(-\Delta) \quad \longrightarrow \quad \Xi = \Phi(bt + c\tau) + e^{\frac{\beta^2(1-p)}{2} - \beta\sqrt{1-p}(bt+c\tau)} \Phi\left(\beta\sqrt{1-p} - bt - c\tau\right) \quad (\text{A20})$$

where $\Phi(x) = \int_x^\infty \mathcal{D}z = \frac{1}{2} \text{erfc}(x/\sqrt{2})$ and for notation's shortness we defined the following three quantities

$$a = \frac{R}{\sqrt{q-R^2}}; \quad b = \sqrt{\frac{q}{1-p}}; \quad c = \sqrt{\frac{p-q}{1-p}} \quad (\text{A21})$$

a. Saddle point equations

The equilibrium behavior of the system at fixed control parameters is given by the maximum of \mathcal{G} w.r.t. all the order parameters, whose values are determined by imposing stationarity of the free energy. After some calculations, we can write the self-consistent equations for the 6 order parameters $R, q, p, \hat{R}, \hat{q}, \hat{p}$ as

$$\hat{R} = \sqrt{\frac{2}{\pi}} \alpha \beta \sqrt{\frac{q}{q - R^2}} \int \mathcal{D}t e^{-\frac{a^2 t^2}{2}} \frac{\int \mathcal{D}\tau \mathcal{T} \Phi(\beta \sqrt{1-p} - bt - c\tau) \Xi^{y-1}}{\int \mathcal{D}\tau \Xi^y} \quad (\text{A22a})$$

$$\hat{q} = 2\alpha\beta^2 \int \mathcal{D}t \Phi(at) \frac{[\int \mathcal{D}\tau \Xi^{y-1} \mathcal{T} \Phi(\beta \sqrt{1-p} - bt - c\tau)]^2}{[\int \mathcal{D}\tau \Xi^y]^2} \quad (\text{A22b})$$

$$\hat{p} = 2\alpha\beta^2 \int \mathcal{D}t \frac{\Phi(at)}{\int \mathcal{D}\tau \Xi^y} \int \mathcal{D}\tau \mathcal{T}^2 \Xi^{y-2} \Phi^2(\beta \sqrt{1-p} - bt - c\tau) \quad (\text{A22c})$$

for the conjugate order parameters (where we defined for convenience $\mathcal{T} = e^{\frac{\beta^2(1-p)}{2} - \beta \sqrt{1-p}(bt+c\tau)}$), and

$$R = \int Dz \Omega(w_1) \quad (\text{A23a})$$

$$q = \int Dz \Omega^2(w_1) \quad (\text{A23b})$$

$$p = \int Dz \Omega(w_1 w_2). \quad (\text{A23c})$$

with

$$\Omega(O) = \frac{1}{\mathcal{Z}_{(y)}(\hat{R}, \hat{p}, \hat{q}, \gamma)} \sum_{w_u \in \pm 1} O \exp \left[\left(\frac{\gamma}{y} + \hat{p} - \hat{q} \right) \sum_{u < v} w_u w_v + \left(\hat{R} + \sqrt{\hat{q}} z \right) \sum_u w_u \right] \quad (\text{A24})$$

with O being a generic observable. It is easy to check that the limit $\gamma \rightarrow 0$ of the free energy (or the saddle point equations) reduces to the non-replicated model, so that all the curves shown in Fig. 2 of the main text for different values of y collapse to the black ones as long as $\gamma \rightarrow 0$.

Appendix B: Simulated Annealing

In this section we discuss the implementation parameters of the simulated annealing (SA). The model (5) is initialized at a temperature T_0 , and each student's weight vector \mathbf{w}_u is drawn at random from $\{-1, 1\}^N$, independently on the others. At each temperature we perform a MonteCarlo sampling using the Metropolis choice for a number of swipes (for each swipe, a move is proposed for all the degrees of freedom). Then the temperature is linearly decreased so that $T_l = T_{l-1} - \eta$ with η a suitable annealing rate. In all the simulations shown in the main text, we used $\eta \in 10^{\{-2, -3, -4, -5\}}$. The standard simulated annealing on a single Perceptron can be easily recovered by setting $\gamma = 0$ in the replicated system: that is equivalent to simulate y Perceptrons independently at the same time. As a final remark, the energy shifts can be efficiently computed using the same procedure discussed in [16] (Supporting Information).